Journal of General Virology (2004), **85**, 3555–3567 DOI 10.1099/vir.0.80379-0

Human cytomegalovirus proteins encoded by UL37 exon 1 protect infected fibroblasts against virus-induced apoptosis and are required for efficient virus replication

Mercedes Reboredo,[1]† Richard F. Greaves[1] and Gabriele Hahn[2]

[1]Department of Virology, Division of Investigative Science, Imperial College Faculty of Medicine, St Mary's Campus, Norfolk Place, London W2 1PG, UK

[2]Max von Pettenkofer Institut, Abteilung für Virologie, LMU-München, Germany

Correspondence
Richard F. Greaves
richard.greaves@imperial.ac.uk

Gabriele Hahn
ghahn@m3401.mpk.med.uni-muenchen.de

Received 18 June 2004
Accepted 25 August 2004

Human cytomegalovirus (HCMV) strain AD169 mutants carrying transposon insertions or large deletions in UL37 exon 1 (UL37x1) were recovered from modified bacterial artificial chromosomes by reconstitution in human fibroblasts expressing the adenovirus anti-apoptotic protein E1B19K. UL37x1 mutant growth was severely compromised in normal fibroblasts, with minimal release of infectious progeny. Growth in E1B19K-expressing cells was restored, but did not reach wild-type levels. Normal fibroblasts infected by UL37x1 mutants underwent apoptosis spontaneously between 48 and 96 h after infection. Apoptosis was inhibited by treatment of cells with the broad-spectrum caspase inhibitor z-Val-Ala-Asp(OMe)-fluoromethylketone, resulting in substantially increased release of virus. Inhibition of viral DNA replication by phosphonoformate or ganciclovir also inhibited apoptosis, implying that death was triggered by late viral functions or by replication and packaging of the viral genome. Immunofluorescent staining showed that although viral proteins accumulated normally during delayed-early phase and viral DNA replication compartments formed, viral late proteins were detected only rarely, suggesting that spontaneous apoptosis occurs early in late phase. These results demonstrate that anti-apoptotic proteins encoded by HCMV UL37x1 [pUL37x1 (vMIA), gpUL37 and gpUL37$_M$] prevent apoptosis that would otherwise be initiated by the replication programme of the virus and are required for efficient and sustainable virus replication.

INTRODUCTION

Apoptosis can compromise the release of viral progeny from infected host cells, thus contributing to innate immunity. Apoptosis may involve activation of extrinsic death receptor-mediated pathways or activation of intrinsic pathways that culminate in the cytoplasmic release of mitochondrial cytochrome *c*, apoptosis-inducing factor and Smac/DIABLO (Benedict *et al.*, 2002; Cory *et al.*, 2003). Extrinsic pathways are triggered by soluble death ligands (e.g. tumour necrosis factor alpha) or by the engagement of cell-surface death receptors by cytotoxic immune cells. Intrinsic pathways are initiated by cellular stress sensors, providing potential systems for viral detection. Apoptotic pathways converge with the cleavage and activation of 'executioner' caspases. Cross-talk between pathways is mediated, for example, by cleavage of the pro-apoptotic Bcl-2 relative, Bid, by extrinsic pathway caspases and its relocalization to mitochondria (Gross *et al.*, 1999). Bid and Bcl-2 are members of a family of mitochondrial proteins that integrate upstream stress and survival signals, regulating apoptosis by controlling mitochondrial membrane integrity (Cory *et al.*, 2003).

Emphasizing the likely role of apoptosis in innate immunity, many viruses encode apoptosis inhibitors (Benedict *et al.*, 2002; Cuconati & White, 2002; Everett & McFadden, 2001), which prevent the premature death of infected cells (Cuconati & White, 2002; Pilder *et al.*, 1984). DNA viruses may have to stimulate the cell cycle to induce a nuclear environment that is conducive to genome replication (Nevins, 1994; White, 2001), but this inappropriate growth stimulus may trigger events – such as p19^{ARF} and p53 activation – that potentiate apoptosis (Debbas & White, 1993; de Stanchina *et al.*, 1998). Human cytomegalovirus (HCMV) infection accordingly drives quiescent fibroblasts into the cell cycle and towards a block in late G_1 or S phase (Bresnahan *et al.*, 1996; Dittmer & Mocarski, 1997; Jault *et al.*, 1995; Lu & Shenk, 1996). HCMV-encoded functions can stimulate (Castillo *et al.*, 2000; Kalejta *et al.*, 2003; Murphy *et al.*, 2000; Poma *et al.*, 1996; Sinclair *et al.*, 2000;

†Present address: Division of Hepatology and Gene Therapy, Department of Internal Medicine, University of Navarra, Pamplona, Spain.

Wiebusch & Hagemeier, 1999) or stall (Lu & Shenk, 1999; Murphy *et al.*, 2000; Noris *et al.*, 2002; Wiebusch & Hagemeier, 1999, 2001) the cell cycle through interactions with cellular proteins (Fortunato *et al.*, 1997; Hagemeier *et al.*, 1994; Kalejta *et al.*, 2003; Margolis *et al.*, 1995; Pajovic *et al.*, 1997; Poma *et al.*, 1996) and the induction of cellular genes (Bresnahan *et al.*, 1998; Song & Stinski, 2002). By subverting normal cell-cycle control, HCMV may optimize conditions for genome replication, but might concurrently stimulate apoptosis.

A functional screen identified several anti-apoptotic proteins that are encoded within the HCMV UL36–38 gene region. The UL37 exon 1 protein (pUL37x1) (termed viral mitochondrion-localized inhibitor of apoptosis or vMIA) blocks apoptosis in response to death-receptor ligation, DNA damage or infection by an E1B-deficient adenovirus (Goldmacher, 2002; Goldmacher *et al.*, 1999). pUL37x1 localizes predominantly to mitochondria and inhibits cytoplasmic cytochrome *c* release. Related glycoproteins (gpUL37 and gpUL37$_M$) that incorporate UL37x1-encoded residues localize partially to mitochondria and have similar, albeit weaker, anti-apoptotic activities (Colberg-Poley *et al.*, 2000; Goldmacher *et al.*, 1999). Two domains (aa 5–34 and 118–147) within the 163 aa pUL37x1 are together both necessary and sufficient for its anti-apoptotic function (Fig. 1a) (Hayajneh *et al.*, 2001). These domains are invariant in clinical strains (Hayajneh *et al.*, 2001) and conserved in functionally homologous primate CMV UL37 proteins (McCormick *et al.*, 2003a). pUL37x1 has no sequence similarity to the cellular apoptotic inhibitor Bcl-2, yet it sequesters the pro-apoptotic Bcl-2 relative Bax in an inactive form in mitochondria (Arnoult *et al.*, 2004). pUL37x1 also binds the adenine nucleotide translocator component of the mitochondrial permeability transition pore (Goldmacher *et al.*, 1999). Expression of pUL37x1 in fibroblasts or HCMV infection disrupts mitochondrial networks (McCormick *et al.*, 2003b). Another unrelated HCMV protein, pUL36 (the viral inhibitor of caspase activation or vICA), inhibits extrinsic apoptotic pathways in an analogous manner to that of viral FLICE-inhibitory proteins or v-FLIPs, preventing activation of caspase 8 in response to death-receptor ligation (Skaletskaya *et al.*, 2001). Immediate-early proteins IE1 p72 and IE2 p86 also have anti-apoptotic properties (Zhu *et al.*, 1995) and IE2 p86 binds and functionally inhibits p53 (Speir *et al.*, 1994).

The UL36–38 locus is transcribed from immediate-early times of infection (Kouzarides *et al.*, 1988; Tenney & Colberg-Poley, 1991), encoding proteins that modulate viral and cellular gene expression (Colberg-Poley *et al.*, 1992, 1998; Iskenderian *et al.*, 1996). Complex transcription, splicing and polyadenylation of the UL36–38 locus (Adair *et al.*, 2003; Kouzarides *et al.*, 1988; Su *et al.*, 2003; Tenney & Colberg-Poley, 1991) produces several major RNA and protein products (Fig. 1b). An immediate-early promoter drives transcription through UL37x1; unspliced messages encode pUL37x1 and messages spliced to UL37x2 and UL37x3 encode gpUL37 or gpUL37$_M$ (Goldmacher *et al.*, 1999). A delayed-early promoter drives transcription

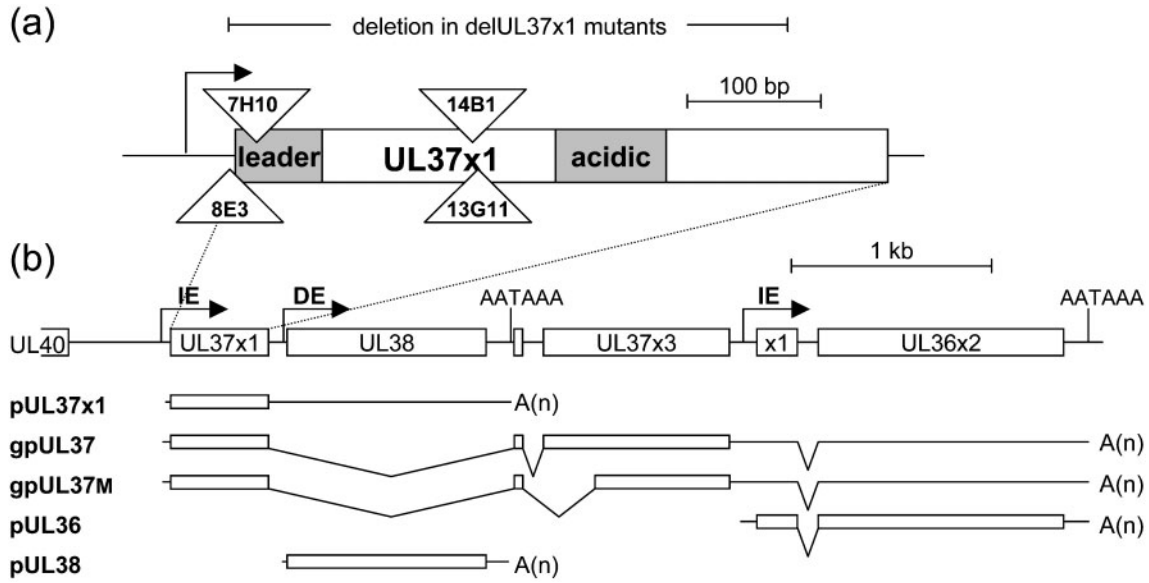

Fig. 1. (a) Scale diagram of the UL37x1 ORF (large box), showing the conserved functional leader and acidic domains (grey boxes), the transcription start site (arrow), mapped insertion points for transposon-insertion mutants RVK8E3, RVK7H10, RVK14B1 and RVK13G11 (triangles) and the extent of the deletion made in delUL37x1 mutants. (b) Scale diagram of the UL36–38 gene locus, showing coding exons (boxes), with immediate-early (IE) and delayed-early (DE) transcription start sites (arrows) and polyadenylation sites (AATAAA). The major coding transcripts from the UL36–38 region are shown below, indicating promoter, exon and polyadenylation site usage.

of the unspliced pUL38 message and a second immediate-early promoter directs transcription of the spliced pUL36 message. pUL37x1 and pUL38 messages share a polyadenylation site and gpUL37, gpUL37$_M$ and pUL36 messages use a second downstream site.

The UL37x1 ORF is well-conserved in all HCMV strains (Hayajneh *et al.*, 2001). Intact gpUL37 is dispensable for virus replication in cultured fibroblasts, demonstrated by deletion of UL37x3 (Borst *et al.*, 1999). Furthermore, several laboratory-adapted strains of HCMV do not encode functional pUL36, revealing this anti-apoptotic function to be inessential (and possibly detrimental) for virus replication in cultured fibroblasts (Skaletskaya *et al.*, 2001). A preliminary report has stated that a virus with a deletion of UL37x1 cannot replicate without the provision of pUL37x1 protein *in trans* (Brune *et al.*, 2003). Recent genomic screens also indicate that UL37x1 is essential for virus growth (Dunn *et al.*, 2003; Yu *et al.*, 2003a).

Here, we have addressed the importance of UL37x1 for the ability of HCMV to replicate in tissue culture by genetic modification. Infection with UL37x1 mutants caused apoptosis of fibroblasts within 4 days, preventing the release of significant quantities of viral progeny.

METHODS

Cell lines. Normal fibroblast MRC5 and GM03468A (NIGMS) cells were maintained as described previously (Borst *et al.*, 1999; Gawn & Greaves, 2002).

Coding sequences for Bcl-X$_L$ and HCMV UL37x1 were PCR-amplified by using *Pfu* polymerase (Stratagene) and primer pairs 5′-GCCGAGATCTATGTCTCAGAGCACCGGGAGC-3′ and 5′-GTACGTCGACTCATTTCCGACTGAAGAGTGAGC-3′ or 5′-GCCGAGATCTATGTCTCCAGTCTACGTGAATC-3′ and 5′-GTACGTCGACTTACTGGTGAGACTGCTGGGG-3′, respectively. UL37x1 was amplified from AD169 cosmid clone pCM1017 (Fleckenstein *et al.*, 1982). A Bcl-X$_L$ cDNA template was provided by Graham Packham (Cancer Sciences Division, University of Southampton, UK). *Bgl*II–*Sal*I fragments ligated into pBabe-Puro (Morgenstern & Land, 1990) produced vectors pRG379 (BclX$_L$) and pRG380 (UL37x1). A *Bam*HI–*Eco*RI–*Xho*I–*Sna*BI–*Mun*I–*Bgl*II–*Sal*I polylinker added to pBabe-Puro produced vector pRG299. An *Eco*RI–*Hin*dIII fragment of plasmid pCMVE1B19K (White *et al.*, 1992) ligated into pRG299 produced vector pRG325. Plasmid pBabe-Puro-bcl2 was a gift from Martin Bennett (Department of Medicine, University of Cambridge, UK).

Retroviral vectors pBabe-bcl2, pRG379, pRG380, pRG325 and pBabe-Puro were packaged in ΦNX-A packaging cells (http://www.stanford.edu/group/nolan/protocols/pro_helper_dep.html), filtered and applied to GM03468A fibroblasts with 5 ng polybrene ml^{-1}. Polyclonally transduced lines were established after 2 weeks puromycin selection (1 μg ml^{-1}). Apoptosis inhibition was confirmed by comparing the responses of transduced populations following 8 h exposure to 1 μM staurosporine with pBabe-Puro-transduced control cells, using terminal transferase dUTP nick end-labelling (TUNEL). Expression of E1B19K was confirmed by using antibody DP07L (Oncogene Research Products).

Mutant bacterial artificial chromosome (BAC) generation and virus culture. BAC DNAs were propagated as described previously (Borst *et al.*, 1999). AD169-BAC carries the full AD169 coding complement and BAC sequences are removed by Cre recombinase during reconstitution, leaving a residual *loxP* site between ORFs US1 and US2 (Hobom *et al.*, 2000). In HB5-BAC, BAC sequences replacing ORFs US2–US6 are retained in reconstituted viruses (Borst *et al.*, 1999). Mutants K8E3, K7H10, K14B1 and K13G11 were isolated from the Tn1721-based Tn*Max8* transposon-insertion mutant library of AD169-BAC (Hobom *et al.*, 2000). Insertion coordinates were sequenced by using universal primer sequences within the Tn*Max8* transposon (Kahrs *et al.*, 1995) and mapped (Chee *et al.*, 1990) at nt 52711 (K8E3), 52688 (K7H10), 52526 (K14B1) and 52522 (K13G11) (Fig. 1a). To construct delUL37x1 mutants by site-directed PCR-based mutagenesis, oligonucleotides were used to amplify pACYC177 DNA (New England Biolabs). The following primers were used: UL37x1for(fko) 5′-**GACTGCTGGGGGCCGTTGTGCTGCAGCATCCGAGCTCGTTGCCGCCGTTGCCACAGGAACCGGTGTCT***CGATTTATTCAACAAAGCCACG*-3′ and UL37x1rev(fko) 5′-**CATCTTCATGTATATAAGACGGTGTTTCAAGACGACGTGAGACCCACACGCGGGTTTCACTTCTTTC***GCCAGTGTTACAACCAATTAACC*-3′ (HCMV homologous sequences are shown in bold and *kan*^{R} homologous sequences in italics). The resulting PCR fragment contained *kan*^{R} flanked by short regions of HCMV homology and was electroporated into DH10B *Escherichia coli* cells containing either AD169-BAC or HB5-BAC and expressing the recombination functions red $\alpha/\beta/\gamma$ (Datsenko & Wanner, 2000; Hahn *et al.*, 2003; Wagner *et al.*, 2002). Colonies were selected on plates containing both kanamycin and chloramphenicol. Viral sequences replaced by *kan*^{R} extended from nt 52293 to 52713 (Chee *et al.*, 1990). Mutant BAC structures were verified by Southern blot analysis.

To reconstitute recombinant viruses, MRC5 cells or GM03468A fibroblasts expressing E1B19K (3468A-E1B19K cells), Bcl-2 or Bcl-X$_L$ were plated into a six-well plate at 70–80 % confluence. The next day, cells were washed in Dulbecco's modified Eagles' medium (DMEM) and incubated in DMEM for 30 min prior to transfection. BAC DNA (1–2 μg) was added to 10 μl SuperFect transfection reagent (Qiagen) and adjusted to 100 μl final volume with DMEM. For AD169-BAC-based mutants, a Cre recombinase-expressing plasmid was added to the transfection (Hobom *et al.*, 2000). After incubation for 30 min at room temperature, 0·9 ml DMEM plus 5 % fetal calf serum (FCS) was added to the transfection mixture. DMEM was removed from the cells and replaced with 1 ml DMEM plus 5 % FCS prior to adding the transfection mix. After incubation for 4 h at 37 °C, the transfection mix was removed and replaced with DMEM plus 5 % FCS for 1 week. Cells were subsequently split into a T25 flask and cultured until appearance of a cytopathic effect (CPE) after approximately 7–10 days. Cultures where no CPE appeared were split and the culture was continued for up to 1 month. For each virus, three to six such independent transfections were performed.

Growth-curve analysis. 3468A-E1B19K or GM03468A cells (5×10^5) were infected with parental virus or UL37x1 mutant viruses (derived from 3468A-E1B19K cells) at an m.o.i. of 0·1 or 3. At the indicated days after infection, viral titres from supernatant media were determined by a standard plaque assay (Greaves & Mocarski, 1998) on 3468A-E1B19K cells.

Protein samples. GM03468A cells (2×10^5) were infected with wild-type parental or UL37x1 mutant viruses at an m.o.i. of 3. At 90 h post-infection (p.i.), viable and detached cells were collected, washed in PBS and lysed directly into 125 mM Tris/HCl, pH 6·8, 2 % SDS. After determination of protein concentration by using the Bio-Rad DC assay, the remaining components of standard SDS-PAGE sample buffer were added. Total protein (10 μg) was subsequently analysed by Western blotting.

TUNEL/fluorescence-activated cell sorter (FACS) assays. GM03468A fibroblasts, 3468A-E1B19K fibroblasts or GM03468A

fibroblasts (4×10^5) transduced with the control retroviral vector pBabe-Puro were infected at an m.o.i. of 3 with viruses harvested from 3468A-E1B19K cells. At 48–96 h p.i., viable and detached cells were pooled, paraformaldehyde-fixed and TUNEL-stained by using an *In Situ* Cell Death Detection kit with fluorescein as indicated by the manufacturer (Roche/Boehringer Mannheim). TUNEL staining was quantified by using a Becton Dickinson FACSort machine. Data were collected, analysed and presented by using CellQuest Pro software. Coverslip-grown cells were similarly fixed and TUNEL-stained *in situ* and then stained with antibody CH167 as described below.

Immunofluorescence analysis. GM03468A fibroblasts (1×10^5) grown on glass coverslips were infected at an m.o.i. of 1 and fixed and permeabilized as described previously (Greaves & Mocarski, 1998). Monolayers were incubated with mAbs at room temperature for 1 h [p63.27 for IE1, CCH2 for ppUL44, M23 for pUL112–113, α-UL69–66 for pUL69, CH167 for pUL57 and 3A12 for pp65; supplied as specified by Gawn & Greaves (2002)] and diluted in PBS plus 10 % FCS as described previously (Gawn & Greaves, 2002), except for CCH2 (DAKO; diluted 1 : 25) and 3A12 (Insight; diluted 1 : 50). PBS-washed cells were then incubated for 1 h with Texas red (Serotec)-conjugated goat anti-mouse Ig for 30 min with PBS/10 % mouse serum and for 1 h with fluorescein isothiocyanate (FITC)-conjugated E13 antibody (Argene-Biosoft) diluted 1 : 50 in PBS/10 % mouse serum. Monolayers were counterstained with Hoechst dye. For the results shown in Table 1, three to four representative fields of 80–130 stained cells were photographed and quantified visually/manually for Hoechst (total cells), FITC (IE protein-positive cells) and Texas red (query antigen) staining.

RESULTS

BACs carrying mutations in UL37x1 fail to reconstitute infectious virus when transfected into normal fibroblasts

Four mutants (Fig. 1a) mapping to UL37x1 were identified in a BAC transposon-insertion library of the AD169 derivative AD169-BAC (Hobom *et al.*, 2000). The Tn*Max8* transposon (from pTSTM8; Brune *et al.*, 1999; Hobom *et al.*, 2000) spans 1·93 kb, including flanking inverted repeats, a resolution site, an origin and a *kan*^{R} gene. Only one transposon mutant (K8E3) generated infectious progeny following transfection of normal human MRC5 fibroblasts. This insertion mapped in the untranslated RNA leader sequence of UL37x1, downstream of the transcription start site (Kouzarides *et al.*, 1988), but 7 nt upstream of the initiation codon. Three non-reconstitutable BACs carried transposon insertions disrupting the UL37x1 ORF (Fig. 1a): K7H10 after aa 5, K14B1 after aa 59 and K13G11 after aa 61. Reconstitution of BACs carrying extensive deletions of UL37x1 in two distinct AD169-derived BACs (AD169-BAC and HB5-BAC) also failed in MRC5 cells. In these delUL37x1 mutants, 420 bp viral sequence spanning 80 % of UL37x1 (encoding aa 1–138 and including the conserved leader and acidic domains) was removed and replaced with a 1·3 kb *kan*^{R} cassette. All reconstitution transfections were attempted in MRC5 cells on at least three occasions and viable progeny were never derived for mutants K7H10, K13G11, K14B1, AD169delUL37x1 or HB5delUL37x1. In contrast, parallel recovery of corresponding wild-type strains and K8E3 was invariably successful. K8E3 virus reconstituted on MRC5 cells was found to still carry the transposon insertion.

To reconstitute UL37x1 mutant viruses, human fibroblast lines designed to resist apoptosis were generated by retroviral transduction, using the cellular genes encoding Bcl-2 and Bcl-X_L or the viral genes encoding adenovirus type 5 E1B19K protein or HCMV pUL37x1. Freshly transduced fibroblast cultures resisted apoptosis after staurosporine treatment, showing negligible TUNEL staining, whilst 30–50 % of control fibroblasts became TUNEL-positive. Only E1B19K-expressing fibroblasts retained staurosporine resistance effectively following long-term culture and displayed the greatest growth potential of these anti-apoptotic lines. These cells were designated 3468A-E1B19K. pUL37x1-expressing cells were particularly difficult to maintain over significant periods in cell culture and were not further utilized. Following antibody staining, 95 % of 3468A-E1B19K cells expressed E1B19K in a perinuclear ring and sometimes also in a fibrous cytoplasmic pattern.

Transfection of fibroblast lines expressing Bcl-2, Bcl-X_L or E1B19K readily resulted in reconstitution of infectious virus from BACs carrying mutations in UL37x1. Infection spread slowly, with 3468A-E1B19K cells yielding the highest-titre stocks. Viral strains reconstituted in 3468A-E1B19K cells were selected for further propagation. Reconstituted virus strains were assigned their BAC designation with the prefix RV, e.g. RVK7H10 or RVAD169delUL37x1. 3468A-E1B19K cells were used for amplification and titration. Mutant stocks were generally 10–100 p.f.u. ml^{-1} lower in titre than corresponding wild-type stocks.

UL37x1 mutant virus strains grow defectively in normal fibroblasts

Multiple-step growth-curve experiments using an input m.o.i. of 0·1 were undertaken for all UL37x1 mutant strains and compared with the corresponding parental virus strains. Growth in 3468A-E1B19K fibroblasts was compared with growth in GM03468A fibroblasts and progeny were plaque-assayed in 3468A-E1B19K cells. Growth of UL37x1 mutants was defective in both cell types (Fig. 2). Mutant strain RVK8E3, which retains an intact UL37x1 ORF, was the least defective of the mutants tested, but still displayed a 10-fold growth deficiency in both cell types (Fig. 2a and b). Transposon mutants RVK7H10, RVK14B1 and RVK13G11 grew weakly in 3468A-E1B19K cells, but did reach output titres slightly higher than the input (Fig. 2a). In contrast, minimal replication was observed for mutants RVK7H10, RVK14B1 and RVK13G11 in GM03468A fibroblasts (Fig. 2b), with progeny titres not approaching input titres, consistent with our failure to reconstitute these virus strains after transfection of normal fibroblasts with the cognate BACs. The deletion mutants RVAD169delUL37x1 and RVHB5delUL37x1 also grew weakly in 3468A-E1B19K cells (Fig. 2c), but did not replicate significantly in GM03468A cultures (Fig. 2d). A

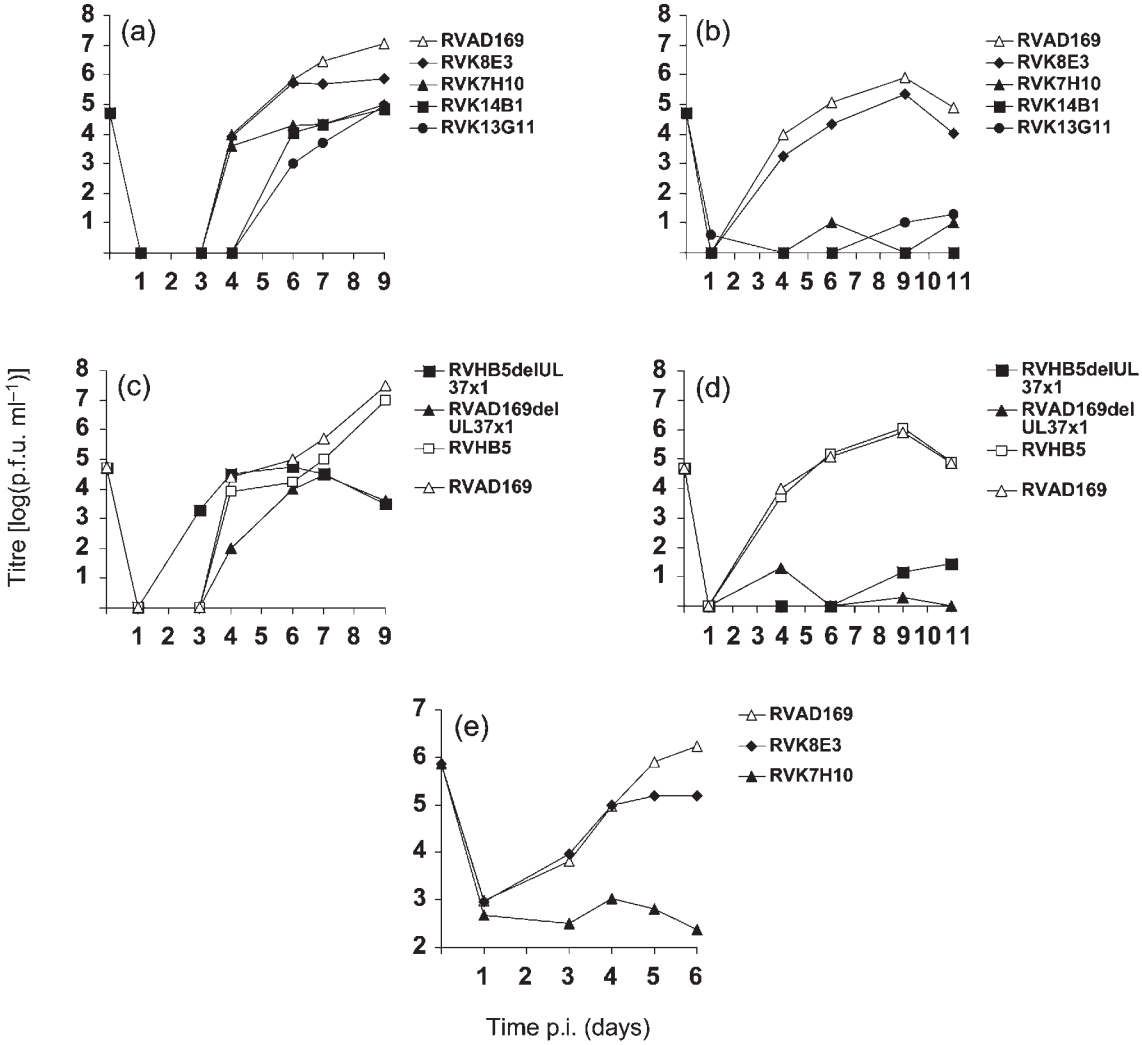

Fig. 2. Growth-curve analysis of UL37x1 mutant viruses and wild-type controls, performed in 3468A-E1B (a, c) or control GM03468A (b, d, e) fibroblasts. (a, b) Transposon-insertion mutants and RVAD169 parental strain (input m.o.i., 0·1). (c, d) delUL37x1 mutants and control parental strains (input m.o.i., 0·1). (e) RVAD169, RVK8E3 and RVK7H10 (input m.o.i., 3). Assays were performed as described in Methods. Data points represent the mean of two independent plaque assays.

single-cycle growth-curve experiment in GM03468A cultures compared RVAD169 with RVK8E3 and RVK7H10 (Fig. 2e). RVK8E3 grew with normal kinetics up to 4 days after infection, but revealed a 10-fold defect in growth at later time points. RVK7H10 replicated extremely poorly, but some virus release was detected after the eclipse phase.

Infection with UL37x1 mutant virus strains causes apoptosis

Extensive cell death was observed during infection by UL37x1 mutant strains. As UL37x1-encoded proteins inhibit apoptosis (Goldmacher, 2002; Goldmacher *et al.*, 1999), we used TUNEL staining to label infected cells containing fragmented chromatin, a defining characteristic of apoptotic cells. TUNEL-stained cells at 96 h p.i. were analysed by FACS (Fig. 3). At this time, most cells in the UL37x1 mutant-infected cultures had detached from the culture vessels. More viable, attached cells remained in cultures infected by mutant RVK8E3, consistent with its intermediate growth phenotype. Most cells infected by wild-type parental strains remained attached. Fig. 3(a–f) shows fluorescence histograms for fibroblasts infected with each mutant (bold curves), in comparison with mock-infected fibroblasts (open curves) and the corresponding parental strain (filled curves). Infected cells showed higher background fluorescence than mock-infected cells, probably due to increased infected-cell volume and associated autofluorescence. All mutant-infected populations showed a high proportion of very brightly staining cells, characteristic of apoptosis. A small reduction was detected in the level of apoptosis in cells infected by the RVK8E3 mutant

(59 %; Fig. 3d), relative to the other three transposon-insertion mutants (88, 83 and 78 %, respectively; Fig. 3a–c), consistent with the increased number of viable cells observed in this culture at time of harvest. A high proportion of TUNEL-positive cells was also observed for the RVHB5delUL37x1 and RVAD169delUL37x1 mutants (68 and 74 %, respectively; Fig. 3e and f). Separate microscopic examination of TUNEL-stained cell suspensions co-stained with Hoechst dye showed that, in all cases, bright TUNEL staining colocalized with chromatin and was often fragmented. TUNEL staining did not colocalize with virus-replication compartments, was not observed in the cytoplasm and was not detected in late-phase cells infected by wild-type virus (Fig. 3g). Therefore, in the context of viral infection, the specificity of TUNEL staining for apoptotic nuclei was not compromised by the presence of viral DNA ends generated by replication and packaging.

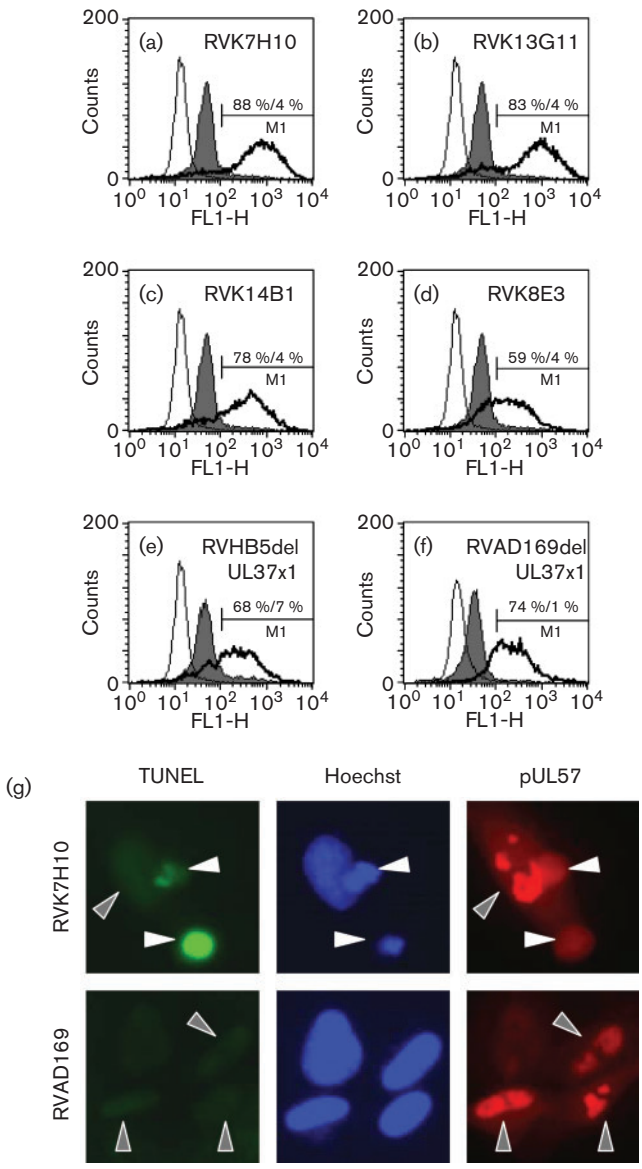

We also compared TUNEL staining in complementing 3468A-E1B cells and control cells infected with the RVK14B1 transposon mutant (Fig. 4a and b). The apoptotic population was reduced, but not abolished (41 % compared with 80 % in control cells) in 3468A-E1B19K cells, consistent with improved survival and propagation of the UL37x1 mutant strains, but correlating with the lack of full growth complementation by these cells.

In a separate experiment, infected cells were incubated with or without the broad-spectrum caspase inhibitor z-Val-Ala-Asp(OMe)-fluoromethylketone (ZVAD-FMK) from 48–96 h p.i. (Fig. 4c and d). ZVAD-FMK abolished TUNEL staining induced by mutant RVK14B1, confirming that caspase-dependent apoptosis gave rise to the TUNEL signal. ZVAD-FMK-treated infected cells remained viable and attached to the culture vessel. A single-step growth curve (Fig. 4e) compared RVAD169 and mutant RVK7H10 in the presence or absence of 50 μM ZVAD-FMK. Replication of RVAD169 was unaffected by ZVAD-FMK treatment, but replication by RVK7H10 recovered substantially by two orders of magnitude, confirming apoptosis as the primary obstacle to UL37x1 mutant replication. A remaining 0·5 log deficit in RVK7H10 replication in the presence of ZVAD-FMK suggested a possible second defect in UL37x1 mutant replication, not attributable to induction of apoptosis.

Apoptosis was measured independently by Western blotting of the 89 kDa fragment of cleaved poly(ADP-ribose) polymerase (PARP) (Fig. 5). In cells infected for 90 h, abundant amounts of cleaved PARP were detected for each of the transposon mutants and for the RVHB5delUL37x1 mutant, compared with mock-infected fibroblasts. Control staurosporine-treated fibroblasts showed a smaller increase in cleaved PARP. Wild-type viruses RVAD169 and RVHB5

Fig. 3. (a–f) FACS analyses of fixed and TUNEL-stained GM03468A fibroblasts, either mock-infected (light curves), infected with the indicated mutant virus (bold curves) or infected with the parental strain RVAD169 (a–d and f) or RVHB5 (e) (filled curves). Cells were infected at an m.o.i. of 3 and harvested 96 h after infection. Plots represent histograms of log(fluorescence intensity) in the FL1 channel for 10 000 cells. Percentage of positive-staining cells in the marked region is indicated for each mutant strain/wild-type control. Fixation, TUNEL staining and FACS analysis were performed as described in Methods. The results of a single experiment are shown in (a–e), whereas (f) was derived from a separate experiment. (g) Human fibroblasts grown on coverslips and infected at an m.o.i. of 3 with RVAD169 wild-type virus or RVK7H10 mutant and fixed at 96 h p.i. Dual staining by TUNEL and anti-pUL57 antibody showed that TUNEL staining (white arrows) was associated with condensed chromatin and a diffuse pUL57 stain. Cells replicating viral DNA, visualized by the characteristic UL57 replication-compartment staining (grey arrows), were not associated with a TUNEL signal during either wild-type or UL37x1 mutant infection.

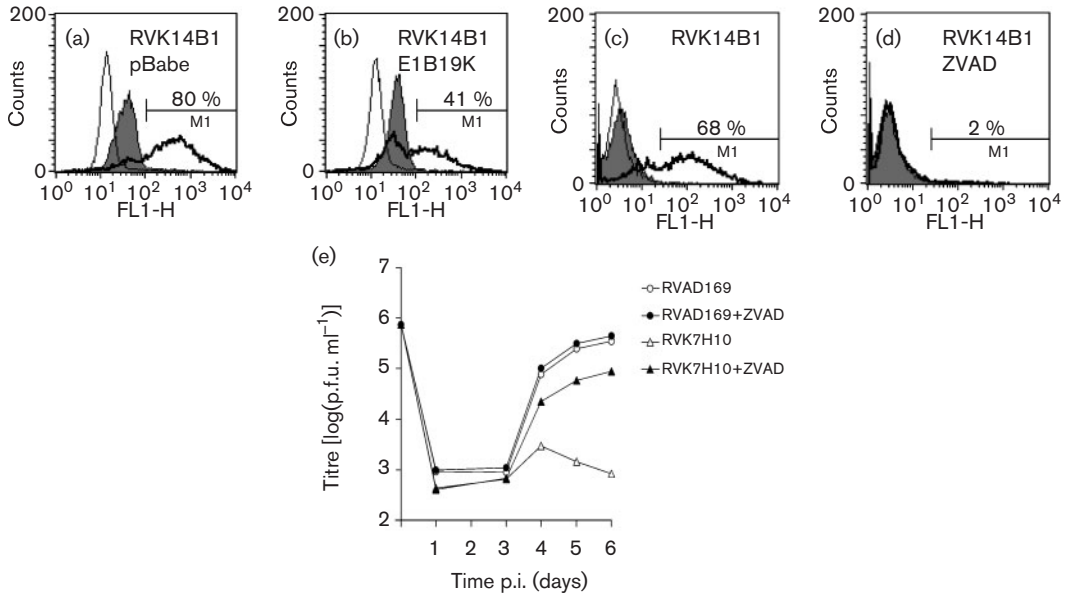

Fig. 4. (a–d) FACS analyses of fixed and TUNEL-stained fibroblasts, either mock-infected (light curves), infected with mutant RVK14B1 (bold curves) or infected with parental strain RVAD169 (filled curves). Cells were infected at an m.o.i. of 3 and harvested 96 h p.i. Plots represent histograms of log(fluorescence intensity) in the FL1 channel for 10 000 cells. (a, b) Experiments conducted in 3468A-E1B19K fibroblast cells (E1B19K) or control pBabe-Puro-transduced GM03468A fibroblasts (pBabe). (c, d) Viruses grown in GM03468A cells in the absence (c) or presence (d) of 50 μM ZVAD-FMK from 48 to 96 h p.i. Percentage of positive-staining cells in the marked region is indicated for RVK14B1. Data in (c) and (d) were collected by using lower FL1 amplification and markers were adjusted correspondingly. Fixation, TUNEL staining and FACS analysis were performed as described in Methods. (e) Single-step growth curve of RVAD169+ZVAD wild-type virus and mutant RVK7H10+ZVAD, carried out in GM03468A cells in the presence and absence of 50 μM ZVAD-FMK. Assays were performed as described in Methods. Data points represent the mean of two independent plaque assays.

showed a very modest increase in cleaved PARP, relative to mock-infected cells. This PARP cleavage assay confirmed that fibroblasts infected by the UL37x1 mutant viruses underwent apoptosis. However, by using this measure, the behaviour of the RVK8E3 mutant was indistinguishable from that of other, more severely growth-compromised mutants.

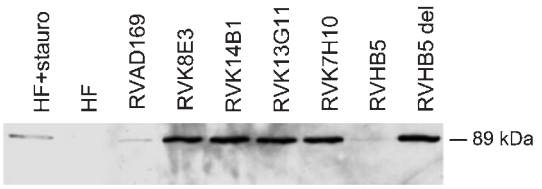

Fig. 5. Western blot analysis of human fibroblast proteins, using an antibody specific for the 89 kDa fragment of cleaved PARP protein. GM03468A fibroblasts were mock-infected (HF), treated for 8 h with 1 μM staurosporine (HF+stauro) or infected at an m.o.i. of 3 with the indicated virus strains for 90 h. Total protein (10 μg) was separated by SDS-PAGE and transferred to nitrocellulose. Blocked membranes were incubated with mAb 19F4 (Cell Signaling Technology), followed by HRP-conjugated anti-mouse Ig and chemiluminescent detection (Amersham Biosciences). Developed film images were digitized on a UMAX Powerlook III flatbed scanner with MagicScan software, followed by brightness adjustment using Adobe Photoshop.

Apoptosis occurs between 48 and 96 h p.i. with UL37x1 mutants and correlates with viral DNA replication

Cells infected with RVHB5UL37x1 were harvested at 48, 72 and 96 h p.i. TUNEL-staining cells were not observed at 48 h (2 %; Fig. 6a), became apparent at 72 h (25 %; Fig. 6b) and peaked at 96 h (76 %; Fig. 6c). Control virus RVHB5 did not induce significant TUNEL staining over this period (Fig. 6c, filled curve). RVHB5delUL37x1-infected cells treated with the viral DNA replication inhibitor phosphonoformate throughout the 96 h infection showed little positive staining (5 %; Fig. 6d). By microscopic examination, drug-treated cells remained attached and apparently viable. In a separate experiment, cells infected by transposon mutant RVK7H10 were incubated for 96 h in the absence and presence of ganciclovir (Fig. 6e and f, respectively). Again, inhibition of viral DNA replication strongly reduced the number of TUNEL-positive cells from 72 to 17 %. These data demonstrated that apoptotic death in cells

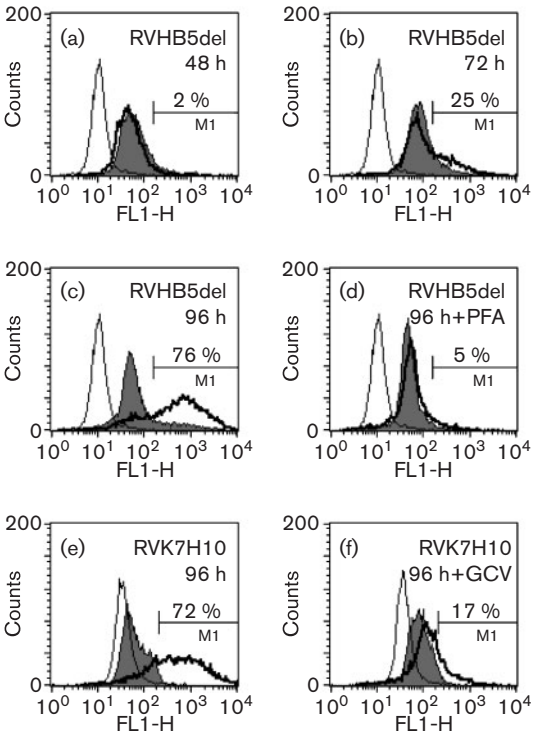

Fig. 6. FACS analyses of fixed and TUNEL-stained fibroblasts, uninfected (open curves), infected with mutant virus (bold curves) or infected with control parental virus strain (filled curves). Cells were harvested at the indicated times p.i. Plots represent histograms of log(fluorescence intensity) in the FL1 channel for 10 000 cells. (a–d) Time course for the RVHB5del37x1 mutant and RVHB5 parental strains grown in GM03468A fibroblasts. Cells analysed in (d) were treated from the time of infection with 200 μg sodium phosphonoformate ml^{-1}. (e, f) Mutant RVK7H10 and parental strain RVAD169 grown in GM03468A fibroblasts in the absence (e) or presence (f) of 400 μM ganciclovir. Data in (e) and (f) were collected by using higher FL1 amplification and markers were adjusted correspondingly. Percentage of positive-staining cells for RVHB5del37x1 or RVK7H10 is presented above the marker used (M1). Fixation, TUNEL staining and FACS analysis were performed as described in Methods.

infected by UL37x1 mutants occurred after 48 h infection and peaked between 72 and 96 h. Apoptosis was dependent on viral DNA replication and/or late-phase progression, as inhibition of viral DNA replication by two mechanistically distinct inhibitors of the viral DNA polymerase strongly inhibited cell death.

UL37x1 mutant-infected cells accumulate delayed-early proteins normally and assemble replication compartments, but late-phase cells are detected extremely rarely

We next investigated the extent to which mutant virus-infected cells proceeded through the replicative cycle. Normal fibroblasts infected by the wild-type strain RVAD169 and mutant strains RVK7H10 and RVAD169delUL37x1 were double-stained at appropriate time points 24–72 h p.i. for IE1/IE2, together with each test antigen. Results are shown in Fig. 7. Unlike the TUNEL and Western blot analyses, the data collected in this experiment excluded detached apoptotic cells. Accumulation of delayed-early pUL112–113, ppUL44, pUL69 and pUL57 occurred in a similar proportion of cells infected by mutant and wild-type viruses, with similar subnuclear localization and intensity of staining. Staining for the ssDNA-binding protein pUL57, characteristic of replication-compartment formation, was seen for all viruses at 60 h p.i. (Fig. 7, arrows). In contrast, cells staining for cytoplasmic pp65 (indicating late-phase progression) at 72 h were much rarer in the mutant virus-infected cultures and generally less bright. Results were quantified by counting stained cells and were related to the proportion of cells co-staining for IE1/IE2 by using antibody E13. These results are shown in Table 1 and emphasize the relative normality of delayed-early phase progression, contrasting with the scarcity of late-phase cells in mutant virus-infected cultures. These data have two potential interpretations: (i) there may be a failure of late gene expression in UL37x1 mutant virus-infected cells; or (ii) the majority of UL37x1 mutant virus-infected cells expressing late proteins may be lost through apoptosis.

DISCUSSION

Our studies have demonstrated that the anti-apoptotic functions encoded within UL37x1 prevent apoptosis that would otherwise occur as a result of virus infection. When UL37x1 mutant viruses infected normal fibroblasts, small numbers of cells reached the late phase of infection and very low levels of progeny virus were detected, well below the input inoculum titres. As characterized by five independent mutants, an intact UL37x1 ORF is therefore required for sustainable virus replication and propagation. By using available antisera to UL37 proteins (Mavinakere & Colberg-Poley, 2004), we could not detect pUL37x1 during normal infection and have not therefore demonstrated loss of the pUL37x1 protein. However, with 80 % of the UL37x1 ORF deleted in delUL37x1 mutants, expression of intact pUL37x1 is theoretically impossible. Furthermore, transposon insertion into mutants RVK7H10, RVK13G11 and RVK14B1 should preclude the assembly of two essential anti-apoptotic domains (Fig. 1a) into one protein. Genetic disruption of UL37x1 will necessarily disrupt gpUL37 and $gpUL37_M$, together with the more abundant pUL37x1 (vMIA). The apoptotic phenotype therefore corresponds with the loss of all three of these anti-apoptotic proteins, although truncated UL37 proteins expressed from exons 2 and 3 may still accumulate. Although UL37x3 is not required for virus replication (Borst *et al.*, 1999), trafficking of gpUL37 and $gpUL37_M$ to different parts of the cell (Colberg-Poley *et al.*, 2000) might conceivably contribute to overall protection against apoptosis. Although our mutations in UL37x1 were not expected to disrupt other

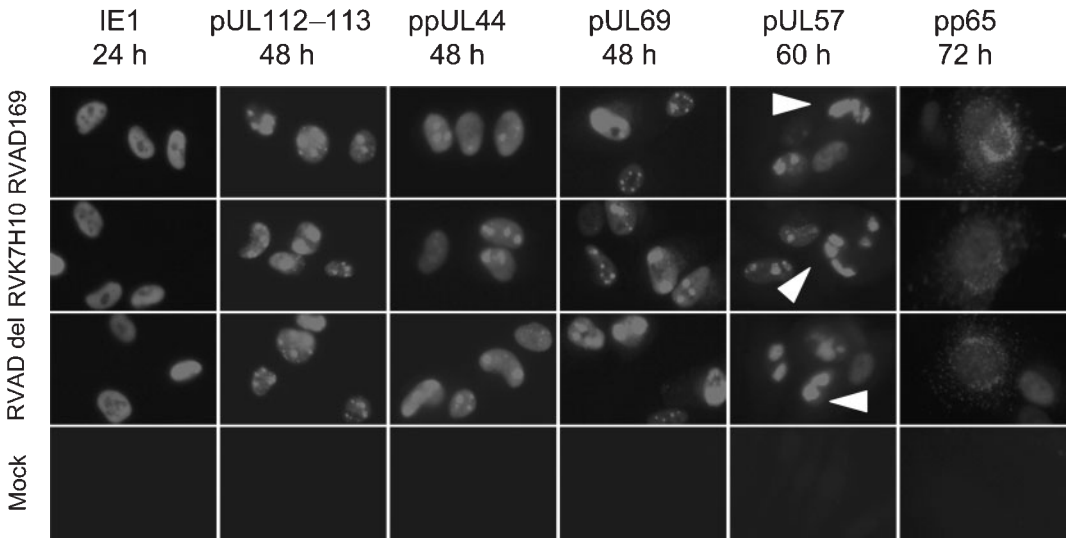

Fig. 7. Immunofluorescence analysis of GM03468A fibroblasts, infected at an m.o.i. of 1 with RVAD169, RVK7H10 or RVAD169delUL37x1 (RVAD del). Panels represent fields of 75 × 50 μm. At indicated times p.i., monolayers were fixed and co-stained for the indicated antigens, combined with antibody E13 to recognize IE1 and IE2 proteins. Photographs show staining for IE1, pUL112–113, ppUL44, pUL69 and pUL57 in representative fields of between four and ten cells. White arrows indicate pUL57 staining in a pattern characteristic of viral DNA replication compartments. Photographs of pp65 staining depict rare positive-staining cells. Images were captured by an Olympus IX-70 fluorescence microscope, via a Hamamatsu C5810 CCD camera and Image Pro Plus software. Brightness and contrast were adjusted for presentation by using Adobe Photoshop software. Images of different virus infections stained with the same antibody were captured and processed identically. Quantitative results of this experiment are presented in Table 1.

promoters or ORFs of the UL36–38 locus, altered expression of other genes – particularly UL38 – might contribute to the growth and apoptosis phenotype that was observed. However, each of these ORFs has been shown to be inessential for HCMV replication (Dunn *et al.*, 2003) and pUL38 is not a known apoptosis inhibitor.

Mutant RVK8E3 had a modest replication defect, but demonstrably induced apoptosis. We propose that timing of apoptosis is key to these differing growth phenotypes. Fully defective UL37x1 mutants apparently induced apoptosis immediately prior to late-phase progression and virus release. A slight delay in the onset of apoptosis in RVK8E3-infected cells, due to residual pUL37x1 expression, could open a short window for virus release and spread, resulting in the observed growth phenotype. In support of this model, E1B19K expression *in trans* delayed, but did not prevent, apoptosis, yet permitted propagation of UL37x1 mutants. Single-cycle growth kinetics in normal fibroblasts revealed that RVK8E3 reached lower peak titres at an earlier time

Table 1. Frequencies of staining for viral antigens after infection at an m.o.i. of 1 by wild-type and UL37x1 mutant viruses

Protein	RVAD169		RVK7H10		RVAD169delUL37x1	
	No. cells stained/ IE-positive/ total counted	Total IE-positive cells (%)/IE-positive cells expressing antigen (%)	No. cells stained/ IE-positive/ total counted	Total IE-positive cells (%)/IE-positive cells expressing antigen (%)	No. cells stained/ IE-positive/ total counted	Total IE-positive cells (%)/IE-positive cells expressing antigen (%)
IE1 (24 h)	141/141/285	49/100	224/224/318	70/100	155/155/326	48/100
pUL112–113 (48 h)	149/167/324	52/89	206/229/311	74/90	142/156/308	51/91
ppUL44 (48 h)	116/178/321	55/65	147/223/326	68/66	81/150/312	48/54
pUL69 (48 h)	104/168/314	54/62	168/209/301	69/80	126/178/349	51/71
pUL57 (60 h)	97/194/317	61/50	96/198/310	64/48	72/137/313	44/53
pp65 (72 h)	19/173/331	52/11	3/199/286	70/1·5	1/152/297	51/0·7

than wild-type virus, consistent with a limited window of virus release. The modestly reduced levels of apoptosis induced by RVK8E3 in a TUNEL assay also supported this model, but such marginal differences in apoptotic potential have not been discernible by other means. A possible discordance between apoptosis induction and replication inhibition queries the significance of apoptosis in the growth phenotype of UL37x1 mutants. However, the caspase inhibitor ZVAD-FMK substantially restored replication of RVK7H10, confirming virus-induced apoptosis as the primary limitation to growth of replication-defective UL37x1 mutant viruses. Partial complementation of the growth of UL37x1 mutants by three independent apoptosis inhibitors (E1B19K, Bcl-2 and Bcl-X_L) also argues that the anti-apoptotic functions of UL37x1-encoded proteins are vital for sustainable virus replication. In contrast, the gammaherpesviruses Epstein–Barr virus (EBV), human herpesvirus 8, murine gammaherpesvirus 68 and herpesvirus saimiri all encode Bcl-2 sequence homologues (Benedict *et al.*, 2002; Cuconati & White, 2002) with related function to pUL37x1, but which for EBV is inessential for latent or lytic virus infection *in vitro* (Marchini *et al.*, 1991).

We studied laboratory strain AD169, whose UL36 inhibitor of caspase activation is non-functional (Skaletskaya *et al.*, 2001). Whilst responses of virus-infected cells to death-receptor ligation will be altered as a result of the absence of UL36 function, AD169 certainly requires an intact UL37x1 gene to protect against infection-initiated apoptosis and to allow sustainable virus replication. It will be informative to analyse UL37x1 mutants constructed against a UL36 wild-type background. pUL36 (vICA) may protect against virus-induced apoptosis in the absence of UL37x1 function; stimulation of death-receptor pathways during the virus late phase could play a role in infection-induced apoptosis. However, we anticipate that the trigger for infection-induced apoptosis is intracellular and that such mutants would also induce apoptosis.

The timing of HCMV-induced apoptosis corresponds with the onset of the late phase of viral gene expression, rather than with virus-induced cell-cycle advance and block. For example, peak cyclin E-associated kinase levels and late G_1/S block have been observed at 24 h after HCMV infection (Bresnahan *et al.*, 1996; Jault *et al.*, 1995; Lu & Shenk, 1996). Induction of apoptosis by adenovirus was formerly thought to occur mainly via E1A-mediated activation of the $p19^{ARF}$–mdm2–p53 pathway and probably via functional induction of the Bcl-2-related Bax protein. However, recent studies question this model. The BH3 protein Bak mediates apoptosis induced by an adenovirus E1B19K mutant in the absence of Bax (Cuconati *et al.*, 2002). Bak is normally sequestered by the MCL-1 protein, which is degraded during adenovirus infection and during the cellular DNA damage response. In the absence of E1B19K, Bak then forms pro-apoptotic complexes with Bax (Cuconati *et al.*, 2003). Other indications suggest that DNA damage could be the primary trigger for apoptosis, either through E1A-induced cellular dysfunction or via viral DNA replication and packaging (Cuconati *et al.*, 2003). Similarly, DNA damage could also be a primary trigger for apoptosis during HCMV infection. As viral polymerase inhibitors blocked HCMV-induced apoptosis, a pro-apoptotic DNA damage signal may result from viral genome replication or packaging. A genetic analysis of host factors required for HCMV-induced apoptosis should determine whether a Bak/MCL-1 mechanism operates similarly to adenovirus or whether other mechanisms – such as p53-mediated synthesis of Bax or BH3-only proteins (Yu *et al.*, 2003b) – are important.

HCMV late-phase functions might induce apoptosis. Pro-apoptotic late proteins may be involved: some viral proteins implicated in HCMV cell-cycle control accumulate to their greatest levels at late times of infection (Kalejta *et al.*, 2003; Lu & Shenk, 1999) and thus might trigger apoptosis. Alternatively, stress induced by accumulation of late-phase viral proteins could trigger apoptosis. Replication of bovine viral diarrhea virus and respiratory syncytial virus both trigger caspase 12-mediated apoptosis via the endoplasmic reticulum (ER) stress pathway (Bitko & Barik, 2001; Jordan *et al.*, 2002) and pUL37x1 can protect against ER stress (Boya *et al.*, 2002).

As UL37 proteins regulate gene expression (Colberg-Poley *et al.*, 1992, 1998), we investigated viral gene expression during infection by UL37x1 mutants. We detected no gross defects in the accumulation of immediate-early or delayed-early proteins, although more sensitive techniques might detect smaller modulations. Our results contrast with observations that UL36–38 products facilitate viral DNA replication (Smith & Pari, 1995), probably due to stimulation of the promoters of viral delayed-early genes (Iskenderian *et al.*, 1996). Specifically, defined UL36–38 transcriptional targets (ppUL44 and pUL57) accumulated normally during UL37x1 mutant infection and viral DNA replication compartments were established normally. However, fewer mutant-infected cells accumulated the viral late protein pp65 at 72 h p.i., probably due to apoptotic loss of cells entering late phase, as accompanied by significant cell death. However, absence of UL37x1 function could also affect late gene expression directly. Indeed, UL37x1 mutant growth was still modestly deficient when apoptosis was inhibited by ZVAD-FMK, suggesting an additional minor growth defect that is not attributable to apoptosis induction.

Our results indicate that UL37x1 expression protects the host cell from apoptosis triggered by virus infection itself. Adequate UL37x1 expression levels are probably essential for maximal apoptosis inhibition. Our preliminary unpublished work indicates that HCMV strains carrying mutations in the major immediate-early gene affect both pUL37x1 expression and the survival time of infected cells. Modulation of UL37x1 may exert sensitive control over the timing of cell death, and regulation of UL37x1 expression may prove to be complex and environmentally responsive. Intriguingly, HCMV may control when its host cell dies.

ACKNOWLEDGEMENTS

This work was supported by MRC Senior (non-clinical) Fellowship G117/314, held by R. F. G. We thank Bodo Plachter, Thomas Stamminger, Markus Wagner, Lenore Pereira, Martin Bennett, Graham Packham, Gary Nolan and Kanji Hirai for gifts of cell lines and reagents used in this study. R. F. G. thanks Richard Caswell, John Sinclair and Paul Farrell for useful discussions. G. H. thanks Dietlind Rose and Sylvia Rhiel for technical assistance.

REFERENCES

Adair, R., Liebisch, G. W. & Colberg-Poley, A. M. (2003). Complex alternative processing of human cytomegalovirus UL37 pre-mRNA. *J Gen Virol* **84**, 3353–3358.

Arnoult, D., Bartle, L. M., Skaletskaya, A., Poncet, D., Zamzami, N., Park, P. U., Sharpe, J., Youle, R. J. & Goldmacher, V. S. (2004). Cytomegalovirus cell death suppressor vMIA blocks Bax- but not Bak-mediated apoptosis by binding and sequestering Bax at mitochondria. *Proc Natl Acad Sci U S A* **101**, 7988–7993.

Benedict, C. A., Norris, P. S. & Ware, C. F. (2002). To kill or be killed: viral evasion of apoptosis. *Nat Immunol* **3**, 1013–1018.

Bitko, V. & Barik, S. (2001). An endoplasmic reticulum-specific stress-activated caspase (caspase-12) is implicated in the apoptosis of A549 epithelial cells by respiratory syncytial virus. *J Cell Biochem* **80**, 441–454.

Borst, E.-M., Hahn, G., Koszinowski, U. H. & Messerle, M. (1999). Cloning of the human cytomegalovirus (HCMV) genome as an infectious bacterial artificial chromosome in *Escherichia coli*: a new approach for construction of HCMV mutants. *J Virol* **73**, 8320–8329.

Boya, P., Cohen, I., Zamzami, N., Vieira, H. L. A. & Kroemer, G. (2002). Endoplasmic reticulum stress-induced cell death requires mitochondrial membrane permeabilization. *Cell Death Differ* **9**, 465–467.

Bresnahan, W. A., Boldogh, I., Thompson, E. A. & Albrecht, T. (1996). Human cytomegalovirus inhibits cellular DNA synthesis and arrests productively infected cells in late G1. *Virology* **224**, 150–160.

Bresnahan, W. A., Albrecht, T. & Thompson, E. A. (1998). The cyclin E promoter is activated by human cytomegalovirus 86-kDa immediate early protein. *J Biol Chem* **273**, 22075–22082.

Brune, W., Ménard, C., Hobom, U., Odenbreit, S., Messerle, M. & Koszinowski, U. H. (1999). Rapid identification of essential and nonessential herpesvirus genes by direct transposon mutagenesis. *Nat Biotechnol* **17**, 360–364.

Brune, W., Nevels, M. & Shenk, T. (2003). Murine cytomegalovirus m41 open reading frame encodes a Golgi-localized antiapoptotic protein. *J Virol* **77**, 11633–11643.

Castillo, J. P., Yurochko, A. D. & Kowalik, T. F. (2000). Role of human cytomegalovirus immediate-early proteins in cell growth control. *J Virol* **74**, 8028–8037.

Chee, M. S., Bankier, A. T., Beck, S. & 12 other authors (1990). Analysis of the protein-coding content of the sequence of human cytomegalovirus strain AD169. *Curr Top Microbiol Immunol* **154**, 125–169.

Colberg-Poley, A. M., Santomenna, L. D., Harlow, P. P., Benfield, P. A. & Tenney, D. J. (1992). Human cytomegalovirus US3 and UL36-38 immediate-early proteins regulate gene expression. *J Virol* **66**, 95–105.

Colberg-Poley, A. M., Huang, L., Soltero, V. E., Iskenderian, A. C., Schumacher, R.-F. & Anders, D. G. (1998). The acidic domain of pUL37x1 and gpUL37 plays a key role in transactivation of HCMV DNA replication gene promoter constructions. *Virology* **246**, 400–408.

Colberg-Poley, A. M., Patel, M. B., Erezo, D. P. P. & Slater, J. E. (2000). Human cytomegalovirus UL37 immediate-early regulatory proteins traffic through the secretory apparatus and to mitochondria. *J Gen Virol* **81**, 1779–1789.

Cory, S., Huang, D. C. S. & Adams, J. M. (2003). The Bcl-2 family: roles in cell survival and oncogenesis. *Oncogene* **22**, 8590–8607.

Cuconati, A. & White, E. (2002). Viral homologs of BCL-2: role of apoptosis in the regulation of virus infection. *Genes Dev* **16**, 2465–2478.

Cuconati, A., Degenhardt, K., Sundararajan, R., Anschel, A. & White, E. (2002). Bak and Bax function to limit adenovirus replication through apoptosis induction. *J Virol* **76**, 4547–4558.

Cuconati, A., Mukherjee, C., Perez, D. & White, E. (2003). DNA damage response and MCL-1 destruction initiate apoptosis in adenovirus-infected cells. *Genes Dev* **17**, 2922–2932.

Datsenko, K. A. & Wanner, B. L. (2000). One-step inactivation of chromosomal genes in *Escherichia coli* K-12 using PCR products. *Proc Natl Acad Sci U S A* **97**, 6640–6645.

Debbas, M. & White, E. (1993). Wild-type p53 mediates apoptosis by E1A, which is inhibited by E1B. *Genes Dev* **7**, 546–554.

de Stanchina, E., McCurrach, M. E., Zindy, F. & 7 other authors (1998). E1A signaling to p53 involves the $p19^{ARF}$ tumor suppressor. *Genes Dev* **12**, 2434–2442.

Dittmer, D. & Mocarski, E. S. (1997). Human cytomegalovirus infection inhibits G_1/S transition. *J Virol* **71**, 1629–1634.

Dunn, W., Chou, C., Li, H., Hai, R., Patterson, D., Stolc, V., Zhu, H. & Liu, F. (2003). Functional profiling of a human cytomegalovirus genome. *Proc Natl Acad Sci U S A* **100**, 14223–14228.

Everett, H. & McFadden, G. (2001). Viruses and apoptosis: meddling with mitochondria. *Virology* **288**, 1–7.

Fleckenstein, B., Muller, I. & Collins, J. (1982). Cloning of the complete human cytomegalovirus genome in cosmids. *Gene* **18**, 39–46.

Fortunato, E. A., Sommer, M. H., Yoder, K. & Spector, D. H. (1997). Identification of domains within the human cytomegalovirus major immediate-early 86-kilodalton protein and the retinoblastoma protein required for physical and functional interaction with each other. *J Virol* **71**, 8176–8185.

Gawn, J. M. & Greaves, R. F. (2002). Absence of IE1 p72 protein function during low-multiplicity infection by human cytomegalovirus results in a broad block to viral delayed-early gene expression. *J Virol* **76**, 4441–4455.

Goldmacher, V. S. (2002). vMIA, a viral inhibitor of apoptosis targeting mitochondria. *Biochimie* **84**, 177–185.

Goldmacher, V. S., Bartle, L. M., Skaletskaya, A. & 10 other authors (1999). A cytomegalovirus-encoded mitochondria-localized inhibitor of apoptosis structurally unrelated to Bcl-2. *Proc Natl Acad Sci U S A* **96**, 12536–12541.

Greaves, R. F. & Mocarski, E. S. (1998). Defective growth correlates with reduced accumulation of a viral DNA replication protein after low-multiplicity infection by a human cytomegalovirus *ie1* mutant. *J Virol* **72**, 366–379.

Gross, A., Yin, X.-M., Wang, K., Wei, M. C., Jockel, J., Milliman, C., Erdjument-Bromage, H., Tempst, P. & Korsmeyer, S. J. (1999). Caspase cleaved BID targets mitochondria and is required for cytochrome *c* release, while $BCL\text{-}X_L$ prevents this release but not tumor necrosis factor-R1/Fas death. *J Biol Chem* **274**, 1156–1163.

Hagemeier, C., Caswell, R., Hayhurst, G., Sinclair, J. & Kouzarides, T. (1994). Functional interaction between the HCMV IE2 transactivator and the retinoblastoma protein. *EMBO J* **13**, 2897–2903.

Hahn, G., Rose, D., Wagner, M., Rhiel, S. & McVoy, M. A. (2003). Cloning of the genomes of human cytomegalovirus strains Toledo, TownevarRIT3, and Towne$_{long}$ as BACs and site-directed mutagenesis using a PCR-based technique. *Virology* **307**, 164–177.

Hayajneh, W. A., Colberg-Poley, A. M., Skaletskaya, A., Bartle, L. M., Lesperance, M. M., Contopoulos-Ioannidis, D. G., Kedersha, N. L. & Goldmacher, V. S. (2001). The sequence and antiapoptotic functional domains of the human cytomegalovirus UL37 exon 1 immediate early protein are conserved in multiple primary strains. *Virology* **279**, 233–240.

Hobom, U., Brune, W., Messerle, M., Hahn, G. & Koszinowski, U. H. (2000). Fast screening procedures for random transposon libraries of cloned herpesvirus genomes: mutational analysis of human cytomegalovirus envelope glycoprotein genes. *J Virol* **74**, 7720–7729.

Iskenderian, A. C., Huang, L., Reilly, A., Stenberg, R. M. & Anders, D. G. (1996). Four of eleven loci required for transient complementation of human cytomegalovirus DNA replication cooperate to activate expression of replication genes. *J Virol* **70**, 383–392.

Jault, F. M., Jault, J.-M., Ruchti, F., Fortunato, E. A., Clark, C., Corbeil, J., Richman, D. D. & Spector, D. H. (1995). Cytomegalovirus infection induces high levels of cyclins, phophorylated Rb, and p53, leading to cell cycle arrest. *J Virol* **69**, 6697–6704.

Jordan, R., Wang, L., Graczyk, T. M., Block, T. M. & Romano, P. R. (2002). Replication of a cytopathic strain of bovine viral diarrhea virus activates PERK and induces endoplasmic reticulum stress-mediated apoptosis of MDBK cells. *J Virol* **76**, 9588–9599.

Kahrs, A. F., Odenbreit, S., Schmitt, W., Heuermann, D., Meyer, T. F. & Haas, R. (1995). An improved Tn*Max* mini-transposon system suitable for sequencing, shuttle mutagenesis and gene fusions. *Gene* **167**, 53–57.

Kalejta, R. F., Bechtel, J. T. & Shenk, T. (2003). Human cytomegalovirus pp71 stimulates cell cycle progression by inducing the proteasome-dependent degradation of the retinoblastoma family of tumor suppressors. *Mol Cell Biol* **23**, 1885–1895.

Kouzarides, T., Bankier, A. T., Satchwell, S. C., Preddy, E. & Barrell, B. G. (1988). An immediate early gene of human cytomegalovirus encodes a potential membrane glycoprotein. *Virology* **165**, 151–164.

Lu, M. & Shenk, T. (1996). Human cytomegalovirus infection inhibits cell cycle progression at multiple points, including the transition from G_1 to S. *J Virol* **70**, 8850–8857.

Lu, M. & Shenk, T. (1999). Human cytomegalovirus UL69 protein induces cells to accumulate in G_1 phase of the cell cycle. *J Virol* **73**, 676–683.

Marchini, A., Tomkinson, B., Cohen, J. I. & Kieff, E. (1991). BHRF1, the Epstein-Barr virus gene with homology to Bcl2, is dispensable for B-lymphocyte transformation and virus replication. *J Virol* **65**, 5991–6000.

Margolis, M. J., Pajovic, S., Wong, E. L., Wade, M., Jupp, R., Nelson, J. A. & Azizkhan, J. C. (1995). Interaction of the 72-kilodalton human cytomegalovirus IE1 gene product with E2F1 coincides with E2F-dependent activation of dihydrofolate reductase transcription. *J Virol* **69**, 7759–7767.

Mavinakere, M. S. & Colberg-Poley, A. M. (2004). Dual targeting of the human cytomegalovirus UL37 exon 1 protein during permissive infection. *J Gen Virol* **85**, 323–329.

McCormick, A. L., Skaletskaya, A., Barry, P. A., Mocarski, E. S. & Goldmacher, V. S. (2003a). Differential function and expression of the viral inhibitor of caspase 8-induced apoptosis (vICA) and the viral mitochondria-localized inhibitor of apoptosis (vMIA) cell death suppressors conserved in primate and rodent cytomegaloviruses. *Virology* **316**, 221–233.

McCormick, A. L., Smith, V. L., Chow, D. & Mocarski, E. S. (2003b). Disruption of mitochondrial networks by the human cytomegalovirus *UL37* gene product viral mitochondrion-localized inhibitor of apoptosis. *J Virol* **77**, 631–641.

Morgenstern, J. P. & Land, H. (1990). Advanced mammalian gene transfer: high titre retroviral vectors with multiple drug selection markers and a complementary helper-free packaging cell line. *Nucleic Acids Res* **18**, 3587–3596.

Murphy, E. A., Streblow, D. N., Nelson, J. A. & Stinski, M. F. (2000). The human cytomegalovirus IE86 protein can block cell cycle progression after inducing transition into the S phase of permissive cells. *J Virol* **74**, 7108–7118.

Nevins, J. R. (1994). Cell cycle targets of the DNA tumor viruses. *Curr Opin Genet Dev* **4**, 130–134.

Noris, E., Zannetti, C., Demurtas, A., Sinclair, J., De Andrea, M., Gariglio, M. & Landolfo, S. (2002). Cell cycle arrest by human cytomegalovirus 86-kDa IE2 protein resembles premature senescence. *J Virol* **76**, 12135–12148.

Pajovic, S., Wong, E. L., Black, A. R. & Azizkhan, J. C. (1997). Identification of a viral kinase that phosphorylates specific E2Fs and pocket proteins. *Mol Cell Biol* **17**, 6459–6464.

Pilder, S., Logan, J. & Shenk, T. (1984). Deletion of the gene encoding the adenovirus 5 early region 1b 21,000-molecular-weight polypeptide leads to degradation of viral and host cell DNA. *J Virol* **52**, 664–671.

Poma, E. E., Kowalik, T. F., Zhu, L., Sinclair, J. H. & Huang, E.-S. (1996). The human cytomegalovirus IE1-72 protein interacts with the cellular p107 protein and relieves p107-mediated transcriptional repression of an E2F-responsive promoter. *J Virol* **70**, 7867–7877.

Sinclair, J., Baillie, J., Bryant, L. & Caswell, R. (2000). Human cytomegalovirus mediates cell cycle progression through G_1 into early S phase in terminally differentiated cells. *J Gen Virol* **81**, 1553–1565.

Skaletskaya, A., Bartle, L. M., Chittenden, T., McCormick, A. L., Mocarski, E. S. & Goldmacher, V. S. (2001). A cytomegalovirus-encoded inhibitor of apoptosis that suppresses caspase-8 activation. *Proc Natl Acad Sci U S A* **98**, 7829–7834.

Smith, J. A. & Pari, G. S. (1995). Expression of human cytomegalovirus UL36 and UL37 genes is required for viral DNA replication. *J Virol* **69**, 1925–1931.

Song, Y.-J. & Stinski, M. F. (2002). Effect of the human cytomegalovirus IE86 protein on expression of E2F-responsive genes: a DNA microarray analysis. *Proc Natl Acad Sci U S A* **99**, 2836–2841.

Speir, E., Modali, R., Huang, E.-S., Leon, M. B., Shawl, F., Finkel, T. & Epstein, S. E. (1994). Potential role of human cytomegalovirus and p53 interaction in coronary restenosis. *Science* **265**, 391–394.

Su, Y., Adair, R., Davis, C. N., DiFronzo, N. L. & Colberg-Poley, A. M. (2003). Convergence of RNA *cis* elements and cellular polyadenylation factors in the regulation of human cytomegalovirus UL37 exon 1 unspliced RNA production. *J Virol* **77**, 12729–12741.

Tenney, D. J. & Colberg-Poley, A. M. (1991). Expression of the human cytomegalovirus UL36–38 immediate early region during permissive infection. *Virology* **182**, 199–210.

Wagner, M., Gutermann, A., Podlech, J., Reddehase, M. J. & Koszinowski, U. H. (2002). Major histocompatibility complex class I allele-specific cooperative and competitive interactions between immune evasion proteins of cytomegalovirus. *J Exp Med* **196**, 805–816.

White, E. (2001). Regulation of the cell cycle and apoptosis by the oncogenes of adenovirus. *Oncogene* **20**, 7836–7846.

White, E., Sabbatini, P., Debbas, M., Wold, W. S. M., Kusher, D. I. & Gooding, L. R. (1992). The 19-kilodalton adenovirus E1B

transforming protein inhibits programmed cell death and prevents cytolysis by tumor necrosis factor α. *Mol Cell Biol* **12**, 2570–2580.

Wiebusch, L. & Hagemeier, C. (1999). Human cytomegalovirus 86-kilodalton IE2 protein blocks cell cycle progression in G_1. *J Virol* **73**, 9274–9283.

Wiebusch, L. & Hagemeier, C. (2001). The human cytomegalovirus immediate early 2 protein dissociates cellular DNA synthesis from cyclin-dependent kinase activation. *EMBO J* **20**, 1086–1098.

Yu, D., Silva, M. C. & Shenk, T. (2003a). Functional map of human cytomegalovirus AD169 defined by global mutational analysis. *Proc Natl Acad Sci U S A* **100**, 12396–12401.

Yu, J., Wang, Z., Kinzler, K. W., Vogelstein, B. & Zhang, L. (2003b). *PUMA* mediates the apoptotic response to p53 in colorectal cancer cells. *Proc Natl Acad Sci U S A* **100**, 1931–1936.

Zhu, H., Shen, Y. & Shenk, T. (1995). Human cytomegalovirus IE1 and IE2 proteins block apoptosis. *J Virol* **69**, 7960–7970.